



Oral Contribution

Powder Pattern Hyperfine Spectroscopy of Shallow-Donor Muonium Centres

H. V. ALBERTO¹, R. C. VILÃO¹, J. PIROTO DUARTE¹, J. M. GIL¹,
N. AYRES DE CAMPOS¹, R. L. LICHTI², E. A. DAVIS³, S. P. COTTRELL⁴
and S. F. J. COX^{4,5,*}

¹*Physics Department, University of Coimbra, P-3004-516 Coimbra, Portugal*

²*Department of Physics, Texas Tech University, Lubbock, Texas 79409-1051, USA*

³*Department of Physics and Astronomy, University of Leicester, Leicester LE1 7RH, UK*

⁴*ISIS Facility, Rutherford Appleton Laboratory, Chilton, Oxfordshire, OX11 0QX, UK*

⁵*Department of Physics and Astronomy, University College London, London WC1E 6BT, UK*

Abstract. The hyperfine spectroscopy of muonium in II–VI semiconductors is reviewed, suggesting that whereas hydrogen is a deep-level defect in ZnS, ZnSe and ZnTe, it constitutes a shallow donor in ZnO, CdS, CdSe and CdTe. Shallow and deep states coexist in CdTe. Using new data for ZnO, it is shown that the principal values of the muonium hyperfine tensor may be obtained with equal facility from measurements in longitudinal or in transverse magnetic field, and from samples that are polycrystalline powders or single crystals. Spin density on the central muon in the shallow states correlates with the electron binding energy or donor depth.

Key words: hydrogen, muonium, shallow donors, ZnO.

The wide-gap II–VI compound semiconductors, already used in solar cell technology, are now on the verge of further important applications as blue light and ultraviolet emitters and other optoelectronic devices. In this paper, we review the hyperfine spectroscopy of muonium centres in this family of compounds which implies that interstitial hydrogen may act as a shallow donor or dopant in at least four of these, namely CdS, CdSe, CdTe and ZnO [1–3]. The ZnO result is in direct confirmation of a recent theoretical prediction [4] and has been reproduced by others [5]. Since hydrogen is an adventitious and unavoidable impurity in all these materials, these new findings have widespread implications for their electronic properties.

In these experiments, muonium is used as an experimentally accessible model for protium, exploiting the sensitivity and timescale of muon spin rotation or relaxation (μ SR) spectroscopy [6]. Highly polarized beams of positive muons are stopped in the sample of interest where they either thermalize as positive ions,

* Speaker and corresponding author.

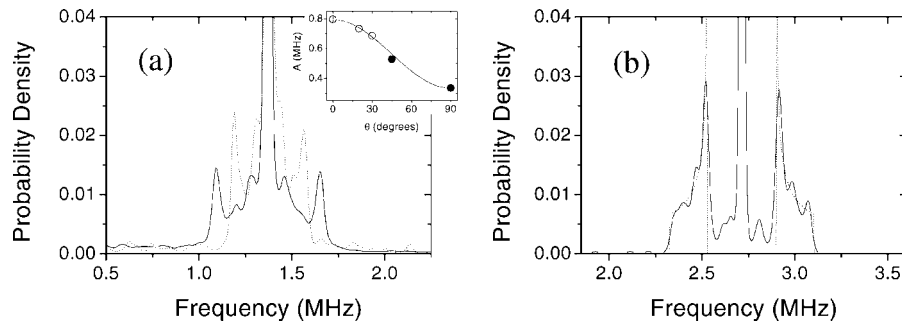


Figure 1. Muon spin rotation spectra for ZnO, recorded at ISIS at 5 K using (a) a single crystal and (b) a powder sample. The transverse magnetic fields were 10 and 20 mT respectively. In (a) the two superimposed spectra correspond to the crystal c -axis oriented at $\theta = 45^\circ$ (full line) and $\theta = 90^\circ$ (dotted line) to the magnetic field. The satellite splittings for these spectra are the solid data points in the insert; the open points for lower values of θ were determined from spectra recorded at PSI. In (b) the lineshape of Equation (1), without additional broadening, is superimposed on the powder spectrum.

mimicking interstitial protons, or else pick up electrons to form atomic muonium ($\text{Mu} = \mu^+e^-$), the light pseudo-isotope of hydrogen. When a magnetic field is applied transverse to the initial muon polarization vector, the polarization precesses under the combined effect of the applied and hyperfine fields. Signals are obtained which resemble NMR free induction decays, but are detected via the asymmetry in the muon radioactive decay. Examples of the frequency transforms of these signals are shown in Figure 1 for single-crystal and powder samples of ZnO. The muons that thermalize as positive ions generate the central line seen in all spectra, at their Larmor precession frequency. (This is 136 kHz/mT – greater than the proton NMR frequency by the ratio of the magnetic moments of these particles, $\mu_\mu/\mu_p = 3.18$.) Those muons that bind an electron during the implantation or thermalization process to form atomic muonium or related defect centres instead show a doublet spectrum, the hyperfine field adding to or subtracting from the applied field according as to whether the electron is initially spin-up or spin-down. The paramagnetic state is then revealed as satellites to the central diamagnetic line. A degree of anisotropy in the paramagnetic state leads to orientation dependence of the splitting in spectra from single crystals (e.g., Figure 1(a)). We find the hyperfine tensors to have axial symmetry in these materials, of the form $(A_\perp, A_\perp, A_\parallel)$ or, equivalently, $(A^* - \frac{1}{2}D, A^* - \frac{1}{2}D, A^* + D)$; in this paper we express the results as the isotropic contact interaction $A^* = \frac{1}{3}(A_\parallel + 2A_\perp)$, which proves always to be the dominant term, and the quantity $D = \frac{2}{3}(A_\parallel - A_\perp)$ which characterizes the smaller traceless dipolar term. The muonium parameters should provide a reliable guide to the electronic structure of protium in these as in other semiconductors, as we describe below, zero-point energy corrections arising from the isotopic mass ratio ($m_\mu/m_p = 0.113$) being small for spectroscopic observables.

Values of these hyperfine parameters measured in single-crystal samples of the four materials are entered in the top half of Table I. The new results for ZnO are

Table 1. Experimental hyperfine parameters for candidate shallow-donor states of muonium: a compendium of results reported to date. Results from single crystal and powder samples, transverse field (TF) and longitudinal field (LF) spectroscopy, are compared for ZnO

Technique	Material	A^* (kHz)	D (kHz)	Reference
Single crystal TF	CdS	244 ± 5	91 ± 6	[1, 3]
Single crystal TF	CdSe	87 ± 4	<40	[2, 3]
Single crystal TF	CdTe	261 ± 4	<50	[2, 3]
Powder TF	ZnO	500 ± 20	260 ± 20	[2, 3]
Single crystal TF	ZnO	502 ± 12	292 ± 12	[5]
Single crystal TF	ZnO	490 ± 10	310 ± 10	this work
Powder TF	ZnO	506 ± 3	270 ± 3	this work
Powder LF	ZnO	457 ± 4	267 ± 6	this work

from a combination of data taken at the ISIS (Oxfordshire) and PSI (Zurich) muon facilities. Referring to Figure 1(a) as an example, these parameters are deduced in the usual fashion from the angular dependence of the splitting between the satellite lines. (We refer here only to the dominant outer satellites. The weaker inner lines are a common feature in our spectra; they do not appear to be transform artefacts but their assignment either to a second paramagnetic state or to splittings of the diamagnetic line by the sparse dipolar nuclei must await further studies.) The spectra were all recorded in the the Paschen–Back régime, even modest fields such as 10 or 20 mT being very much greater than the hyperfine field $2\pi A^*/\gamma_e$; we show below that nuclear superhyperfine interactions are also well decoupled at these fields and cannot contribute any broadening or splitting of the transverse-field spectra.

The anisotropy of the hyperfine coupling is not severe for these muonium states so that, with polycrystalline samples, the muon spin rotation spectra are not broadened beyond detection. On the contrary, distinctive powder-pattern spectra are readily observed, as in Figure 1(b). Here we fit the satellite lineshapes with a function derived from the probability density of the precession frequency distribution $dP/d\nu$ expected for a random distribution of the angle θ between the symmetry axis of the hyperfine interaction tensor and the externally applied field:

$$\frac{dP}{d\nu} = \frac{dP}{d\theta} \frac{d\theta}{d\nu} = (3D/2)^{-1/2} (2(|\nu - \nu_0| - A^*/2) + D/2)^{-1/2}$$

$$\text{for } \nu_0 - A_{\parallel}/2 \leq \nu \leq \nu_0 - A_{\perp}/2 \text{ and } \nu_0 + A_{\perp}/2 \leq \nu \leq \nu_0 + A_{\parallel}/2, \quad (1)$$

where ν_0 is the centre of the distribution, usually coincident with the Larmor precession frequency of the diamagnetic muon state. The form of the powder pattern shows that the inner splitting must correspond to A_{\perp} , corresponding to the most

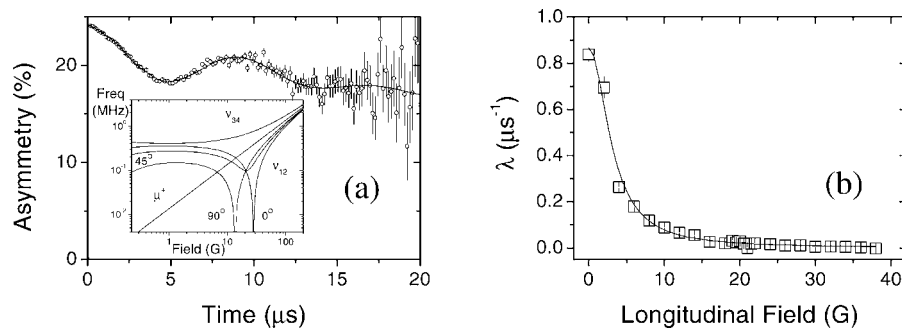


Figure 2. Muon spin response function at the “magic” longitudinal field of 2.0 mT (a) and the suppression of cross-relaxation rate λ to neighbouring ^{67}Zn nuclei as a function of longitudinal decoupling field (b).

probable value of θ , and the outer to A_{\parallel} . The results of the fit for the parameters A^* and D , somewhat more precise than those reported earlier [3], are entered in the lower half of Table I.

We now examine the muon response in longitudinal fields, i.e., magnetic fields applied parallel to the initial beam polarization. The signals are obtained directly from the muon decay asymmetry without field-switching techniques since, contrary to conventional magnetic resonance, no polarizing field is required in μSR experiments either to prepare or analyse the muon polarization. In null external field, the signal is the combined response to the muon hyperfine interaction and superhyperfine interactions with neighbouring dipolar nuclei. These latter are sparse in ZnO (the natural abundance of ^{67}Zn nuclei is just 4%) but the extension of the electron wavefunctions means that a broad distribution of superhyperfine couplings is to be expected. More readily interpreted is the signal at the so-called magic field given by $\pi A^*/\gamma_{\mu}$, corresponding to an anticrossing in the muonium energy level diagram [6]. Here a particular transition frequency coincides for crystallites of all possible orientations. (Magic-field signals have been used previously to detect highly anisotropic bond-centred muonium in diamond, albeit for kinetic rather than spectroscopic studies [6].) For ZnO, this field falls close to 2 mT, at which point the superhyperfine interactions are sufficiently decoupled for the oscillations to be quite distinct. The signal, recorded at ISIS, is shown in Figure 2(a). Our fitting function is generated from all the contributing transitions within the energy-level diagram, again as an appropriate polycrystalline average. The fitted values of A^* and D are entered in the lower half of Table I. They lie within 10% of those obtained by transverse field spectroscopy, single crystal and polycrystalline. The small discrepancy may be attributed to inadequate modelling of the ^{67}Zn superhyperfine interactions, which still contribute to the longitudinal field response at the magic field. (The transverse-field precession signals of Figure 1, on the other hand, were recorded well into the Paschen–Back, or decoupled, régime and are sensitive to the muon–electron hyperfine interaction only.) Adding an empirical

term to the fitting function to account for this, in the form of an exponential term representing cross relaxation to the ^{67}Zn nuclei, longitudinal-field signals can be fitted over a wide range of fields. We find the cross-relaxation rate to be suppressed as a Lorentzian function of field with a half-width of 0.63 ± 0.03 mT. This is shown in Figure 2(b). We hope in due course to use these nuclear couplings to map the spatial distribution of spin density, confirming the extent of the electron wavefunction.

These spectra, whether in transverse or longitudinal field, do not in themselves determine which interstitial site or sites the muon occupies. From the similarity of the spectra in material of different origin we can at least reasonably exclude defect-related sites. Despite the convenience of powder pattern spectroscopy in giving both principal values of the hyperfine tensor from a single spectrum, single crystals studied in a number of orientations are necessary to determine the crystallographic direction of the symmetry axis. Our data show it to lie along the crystal c -axis, which is the direction of one of the two inequivalent bond directions in the hexagonal wurtzite lattice. The two likely sites are close to the bond centre and antibonding to oxygen. Van de Walle finds these to have similar energy for the interstitial proton, with the bond-centre site between anion and cation slightly the more stable [4]; however, by analogy with our muon site determination in CdS, albeit in the dissociated or ionized state, we favour the site which is antibonding to the anion [1, 3] and which – for the c -axis sites – is constrained within a cage of the wurtzite structure. Somewhat surprisingly, but consistent with the findings of others (Shimamura *et al.* [5] found $A_{\parallel} = 795 \pm 15$, $A_{\perp} = 356 \pm 4$ kHz from single crystal studies of ZnO; these authors also report a second state, apparently with a much lower binding energy, with $A_{\parallel} = 579 \pm 15$, $A_{\perp} = 150 \pm 4$ kHz), the analogous sites related to the off-axis bonds do not appear to be populated in proportion to their number, if at all. These off-axis antibonding sites lie in more open channels in the structure so that any motion or tunnelling between them would give a partial narrowing of anisotropic parameters. It may be that the small features with intermediate splittings in the spectra of Figure 1 represent some degree of occupancy of these sites, but given the high (4 MeV) muon implantation energy, and the resultant tendency to populate metastable states of comparable energy, this chemical preference for cage sites on thermalization is remarkable. Clues to the nature of the local bonding are perhaps to be found in the values of the anisotropy parameter D , which we note are larger, in CdS and ZnO at least, than can be explained from anisotropy in the bulk electronic parameters, dielectric constant ϵ or electron effective mass m^*/m_e .

Finally we comment and enlarge on the physical conclusions of this spectroscopy. We recall that hydrogen is commonly regarded as a deep-level or compensating defect. Accordingly, only muonium states with compact electron wavefunctions are seen in the elemental Group IV and compound III–V semiconductors; even in the II–VI compounds ZnS and ZnSe, the muonium electron is strongly bound and the hyperfine constant is some 80% of its vacuum-state value [6]. Our own

recent experiments confirm the older ZnS and ZnSe results and likewise suggest a similarly deep state in ZnTe, without revealing any coexisting shallow state in any of these three compounds. Amongst the zinc chalcogenides, ZnO is therefore unique in showing the shallow state. The signals from this and its diamagnetic or dissociated counterpart (presumably Mu^+ , although we cannot totally exclude the hydride ion analogue $\text{Mu}^- = \mu^+ e^- e^-$ in this naturally n-type material) together account for all the incoming muon polarization, so no deep state coexists in ZnO. Of the II–VI compounds so far studied, only CdTe shows coexisting deep and shallow states.

For all four materials in Table I the contact terms A^* , representing electronic spin density on the muon, are some four orders of magnitude smaller than the hyperfine constant of vacuum-state muonium ($A_0 = 4.5$ GHz). It is this factor which is suggestive of weakly bound electrons with extended wavefunctions. The effective Bohr radii inferred from these spin densities are comparable with values calculated within the effective-mass model [3]; ionization temperatures and activation energies deduced from the temperature dependence of signal amplitudes are also consistent with the shallow-donor interpretation [1–3]. Here we reinforce this interpretation by noting a relationship between central spin density and ionization energy. In the usual notation, we combine the effective-mass expressions $a^* = a_0 \varepsilon / (m^*/m_e)$, $R^* = R_0 (m^*/m_e) / \varepsilon^2$ and $A^* = A_0 (a_0/a^*)^3$ to give

$$R^* = \frac{R_0}{\varepsilon} \left(\frac{A^*}{A_0} \right)^{1/3} \quad (2)$$

with $R_0 = 13.6$ eV. (The electron reduced masses and vacuum-state Rydberg constants or binding energies are the same for muonium and protium to within a fraction of a percent.) These values are compared in Table II with the experimental binding energies. Given the usual corrections which need to be applied to the effective mass model, the order-of-magnitude agreement is strongly supportive of the shallow-donor model.

In conclusion, we have demonstrated that muonium hyperfine parameters can be obtained from longitudinal as well as transverse-field spectroscopy, using pow-

Table II. Correlation of spin density on the central muon, converted to the effective Rydberg constant via Equation (2), with experimental donor-level depth (these latter from references [2, 3])

	A^*/A_0	R^* (meV)	E_d (meV)
CdS	0.55×10^{-4}	59	26 ± 6
CdSe	0.19×10^{-4}	37	20 ± 4
CdTe	0.58×10^{-4}	52	16 ± 4
ZnO	1.1×10^{-4}	79	58 ± 6

der samples as well as single crystals. Powder pattern hyperfine spectroscopy has scarcely been used previously in μ SR experiments but it is clear that with the quality and intensity of muon beams now available, and in this case also benefitting from the background-free spectra obtainable at the ISIS pulsed source, it is quite feasible for these relatively narrow spectra. This should greatly facilitate the search for these shallow-donor states of muonium in other semiconductors. The powder signals will also be perfectly suitable for studies of the thermal stability and ionization characteristics of these states, as well as their interaction with charge carriers from other defects or dopants.

Acknowledgements

These experiments are supported by EPSRC grant GR/R25361 (United Kingdom) and FCT/POCTI grant 35334/FIS/2000 (Portugal). Discussions with A. Weidinger and K. Shimamura are gratefully acknowledged.

References

1. Gil, J. M., Alberto, H. V., Vilão, R. C., Pioto-Duarte, J., Mendes, P. J., Ferreira, L. P., de Campos, A. N., Weidinger, A., Krauser, J., Niedermayer, Ch. and Cox, S. F. J., *Phys. Rev. Lett.* **83** (1999), 5294.
2. Cox, S. F. J., Davis, E. A., Cottrell, S. P., King, P. J. C., Lord, J. S., Gil, J. M., Alberto, H. V., Vilão, R. C., Pioto-Duarte, J., de Campos, A. N., Weidinger, A., Lichti, R. L. and Irvine, S. J. C., *Phys. Rev. Lett.* **86** (2001), 2601.
3. Gil, J. M., Alberto, H. V., Vilão, R. C., Pioto-Duarte, J., de Campos, N. A., Weidinger, A., Krauser, J., Davis, E. A., Cottrell, S. P. and Cox, S. F. J., *Phys. Rev. B* **64** (2001), 075205.
4. Van de Walle, C. G., *Phys. Rev. Lett.* **85** (2000), 1012.
5. Shimamura, K., Nishiyama, K. and Kadono, R., In: *International Conference on Defects in Semiconductors*, Giessen, July 2001; *Phys. B* (in press).
6. Patterson, B. D., *Rev. Mod. Phys.* **60** (1988), 69.